Analytical and Bioanalytical Chemistry
https://doi.org/10.1007/s00216-018-1443-6

RESEARCH PAPER

Tunable superamphiphobic surfaces: a platform for naked-eye ATP detection

Fujian Huang [1] · Yan Chen [1] · Yongqian Wang [1] · Fan Xia [1,2]

Received: 18 July 2018 / Revised: 24 September 2018 / Accepted: 22 October 2018

Abstract

A superamphiphobic surface composed of two different size ranges of TiO_2 nanoparticles was simply fabricated through spraying the perfluorosilane coated TiO_2 nanoparticles suspension dispersing in ethanol. The surface chemistry was finely regulated through gradient UV irradiation-induced organic compound degradation to fabricate surface with gradient solid surface energy or wettability. The fabricated surface shows good droplet sorting ability, which can successfully discriminate ethanol droplets with different concentrations. As a proof-of-concept, the biosensor application of this surface was demonstrated by using it for naked-eye ATP detection. Liquid droplets with different concentrations of ATP after ATP-dependent rolling circle amplification (RCA) can be effectively sorted by the surface. This developed biosensor methodology based on droplet sorting ability of the fabricated surface is energy-efficient and economical which is promising for biosensors, point-of-care testing, and biochemical assays.

Keywords Biosensor · Superamphiphobic surface · Droplet sorting · ATP detection · Point-of-care testing

Introduction

In recent years, surfaces with special wettability are desirable because of their widespread applications, including self-cleaning [1–3], antifouling [4], anti-icing [5–7], liquid separation [8, 9], droplet bouncing [10, 11], droplet manipulations [12, 13], and droplet sorting [14]. As far as we know, there are a few reports that indicate surface with special wettability that can be directly used for naked-eye biosensor applications.

For the naked-eye sensing format, colorimetric sensors have attracted considerable interest because of their simple- and instrument-free characteristics. Colorimetric ELISA [15] and plasmonic nanoparticles-based colorimetric assay [16, 17] are the two most used colorimetric naked-eye diagnostic techniques. Traditional naked-eye sensing strategies based on the color change of the assays are more or less suffer from insensitive to the shading of a color, which limits the sensitivity of the detection [18]. Herein, we propose a new concept for the naked-eye biosensor based on the different rolling ability of droplets with different physicochemical property on the tunable superamphiphobic surface.

As tunable superamphiphobic surfaces have been applied in many fields, the fabrication of such surfaces with patterned or gradient wettability is a crucial step in practical relevant applications. To date, many technologies and methods have been developed to fabricate patterned wettability on superhydrophobic surfaces, including ink printing [19], soft-lithography [20], and photolithography [21, 22]. Most of current methods are focused on the preparation of patterned wettability on superhydrophobic surfaces. It is desirable to fabricate wettability gradient on superomniphibic surfaces for biosensor applications.

In this study, we aimed to fabricate tunable superamphiphobic surfaces composed of TiO_2 nanoparticles for biosensor applications. TiO_2 with high photocatalytic efficiency could be used to

Published in the topical collection *Young Investigators in (Bio-)Analytical Chemistry* with guest editors Erin Baker, Kerstin Leopold, Francesco Ricci, and Wei Wang.

Fujian Huang and Yan Chen contributed equally to this work.

Electronic supplementary material The online version of this article (https://doi.org/10.1007/s00216-018-1443-6) contains supplementary material, which is available to authorized users.

✉ Fan Xia
xiafan@hust.edu.cn

[1] Engineering Research Center of Nano-Geomaterials of Ministry of Education, Faculty of Materials Science and Chemistry, China University of Geosciences, Wuhan 430074, Hubei, China

[2] Hubei Key Laboratory of Bioinorganic Chemistry & Materia Medica, Huazhong University of Science and Technology, Wuhan 430074, Hubei, China

Published online: 10 November 2018

regulate the chemical composition of the surface, and thus tune the solid surface energy under UV irradiation. It was proved that the solid surface energy could be gradiently regulated through gradient UV irradiation. The liquid droplet-sorting ability of the superamphiphobic surfaces with gradient solid surface energy was demonstrated and the possibility for biosensor application was studied. To our best knowledge, this is the first report of using superamphiphobic surfaces with gradient wettability to detect biomolecules.

Experimental section

Materials

1H, 1H, 2H, 2H-perfluorooctyltriethoxysilane (98%) and titanium (IV) oxide were purchased from Sigma-Aldrich. P25 titanium oxide was purchased from Degussa. Laboratory solvent, ethanol absolute was purchased from Sinopharm. Phosphorylated linear ssDNA and primer probes were purchased from Shanghai Sangon Biotech. T4 DNA ligase, phi29 DNA polymerase, and 5 × TBE buffer were purchased from Thermo Scientific. Deoxyribonucleoside 5′-triphosphates mixture (dNTPs) was purchased from Sigma-Aldrich. ATP, AMP, GTP, CTP, and UTP were purchased from BBI Life Science. Gel Red was purchased from Biotium.

Fabrication of superamphiphobic surface

0.2 g 1H, 1H, 2H, 2H-perfluorooctyltriethoxysilane was added into 19.8 g ethanol absolute, and the solution was mechanically stirred for 2 h. Then, 1.2 g titanium (IV) oxide and 1.2 g P25 were added into solution; the suspension was mechanically stirred for overnight to make a uniform suspension. The glass (50 mm × 50 mm × 3 mm thick) was pretreated by ultrasonicating for 10 min in acetone, ethanol, and ultrapure water, respectively, and drying with drier. The uniform suspension is painted on the pretreated glass by spray gun (Lotus, Shanghai) with a 0.8-mm nozzle diameter by using a nitrogen pressure source with flow of 10 L/min. Then, the painted glass was dried in air horizontally.

Regulating the solid surface energy of superamphiphobic surface

The solid surface energy of superomniphibic surface was continuously tuned by manipulating an injection pump with a lightproof mask moving at a velocity of 2.5 mm/min for acquiring different UV irradiation time of the surface. The UV area light source is an UV-LED lamp ($\lambda = 365$ nm) with 10 cm long and 10 cm wide. The paint is placed approximately 20 cm away from the UV-LED lamp. The UV light intensity irradiated on the surface was about 1300 $\mu W/cm^2$.

Characterization of the fabricated surface

The X-ray diffraction (XRD) patterns are performed on a D8 Advance Diffractometer (Bruker Corporation, Germany) with Cu Kα radiation ($\lambda = 1.54178$ Å) at a scanning rate of 0.02° s^{-1} in the 2θ range from 10° to 80°. The morphology of samples is characterized by a Hitachi SU8010 Field Emission Scanning Electron Microscopy (FESEM, Japan). X-ray photoelectron spectroscopy (XPS, USA) was operated by Thermo Scientific VG ESCALAB 250 photoelectron spectrometer through the Al Kα line as the excitation source at an energy step size of 0.1 eV. High-resolution scans were done for the F (1 s), Ti (2p), O (1 s), Si (2p), and C (1 s) at a pass energy of 20 eV. The contact angles were measured at room temperature via the sessile-drop method using an optical contact angle goniometer OCA20 (Dataphysics, Germany). The video of the movement of different droplets is recorded by contact angle goniometer DSA100 (Kruss) with 200 fps.

Rolling circle amplification

One microliter of phosphorylated linear ssDNA (30 μM) is mixed with 3 μL of primer probes (30 μM) in 36 μL hybridization buffer (pH 7.5, 10 mM Tris-HCl, 100 mM NaCl, 5 mM $MgCl_2$). The mixture solution was heated to 95 °C for 10 min and then slowly cooled down to room temperature. Then, 10 μL of T4 DNA ligase, 10 μL T4 DNA ligase buffer (pH 7.8, 400 mM Tris-HCl, 100 mM $MgCl_2$, 100 mM DTT, 5 mM ATP), and 40 μL sterile ultrapure water was added into solution and incubated at 37 °C for 2 h to produce circular DNA templates. The T4 ligase buffer contains different concentrations of ATP, 5 mM AMP, 5 mM GTP, 5 mM UTP, and 5 mM CTP for ATP detection and specificity detection, respectively. After the ligation, T4 DNA ligase was inactivated at 65 °C for 10 min. Then, the circular DNA templates of 50 μL was performed with 2 μL phi29 DNA polymerase (1 unit/μL), 10 μL phi29 DNA polymerase buffer (pH 7.9, 330 mM Tris-acetate, 100 mM Mg-acetate, 660 mM K-acetate, 10 mM DTT) 18 μL sterile ultrapure water and 20 μL dNTP (25 mM) at 37 °C for 1 h. The resulting solution was heated to 65 °C for 10 min to inactivate the DNA polymerase before measurement.

Gel electrophoresis

The products of RCA were analyzed by using 0.9% agarose gel electrophoresis. A potential of 130 V at 25 °C for 110 min was applied for gel electrophoresis separation with 1 × TBE buffer. After separation, agarose gel was analyzed by gel image system Tanon-5200 Multi (Tanon, China).

Results and discussion

The principles for biosensing applications

The principles for biosensing applications in our system is based on the droplet sorting capacity occur on the superamphiphobic surfaces with gradient solid surface energy. Superamphiphobic surfaces are surfaces which are both superoleophobic and superhydrophobic. Liquid droplets can easily roll off from the superamphiphobic surfaces due to the high apparent contact angle θ^* (usually $\theta^* > 150°$) and low contact angle hysteresis $\Delta\theta^*$ (usually $\Delta\theta^* < 10°$) [23]. When the droplets roll off from the tilted surfaces with a fixed angle, there would be a balance between work done due to gravity and work expanded because of adhesion as descripted in Eq. 1.

$$\rho g V \sin\omega \approx \gamma_{lv} D_{TCL} (\cos\theta^*_{rec} - \cos\theta^*_{adv}) \quad (1)$$

where, ρ is the density of the liquid, g is the acceleration of gravity, V is the volume of the liquid droplet, ω is the roll off angle of the droplet (the minimum angle the surface must be tilted for droplet to roll off). D_{TCL} is the width of solid-liquid-vapor contact line perpendicular to the rolling direction, θ^*_{rec} and θ^*_{adv} are the apparent receding and advancing contact angles, γ_{lv} represents the interaction between liquid and solid surface.

In the case of droplets with fixed volume but different surface intense (or different interaction between liquid and solid surface), droplets with lower γ_{lv} (or stronger interaction with solid surface) adhere more to a superamphiphobic surface which results in a higher D_{TCL} and higher $\Delta\theta^*$, and then display higher ω. For the liquid droplets with higher γ_{lv} (or weaker interaction with solid surface), the droplets adhere less to the superamphiphobic surface and display a lower ω. Thus, it could be predicted that liquid droplets with certain higher surface tension (or weaker interaction with solid surface) will roll off from the solid surface with certain surface energy γ_{sv} and appropriate tilt angle α (here $\omega < \alpha$), while droplets with lower surface tension and $\omega > \alpha$ will adhere to the surface. Accordingly, when droplets with different surface tensions (or different interaction with solid surface) were placed on the superamphiphobic surface with identical surface structure and fixed tilt angle α, but different or gradient solid surface energy, droplets with higher surface tension could be more likely to roll off from the surface while droplets with lower surface tension tend to adhere on the surface, which means that, at a fixed tilt angle α, the superamphiphobic surface with lower solid surface energy will allow more liquids with appropriate surface tension to roll off from the surface compared to the one with higher solid surface energy. In this way, the superamphiphobic surface with fixed tilt angle α and gradient wettability (or solid surface energy) could be used to sort droplets with different surface tensions (or different interaction with solid surface). When the liquid droplets roll off from the top edge (edge with lower solid surface energy) of the superamphiphobic surface at a fixed tilt angle α and gradient solid surface energy, droplet with lower surface tension (or stronger interaction with solid surface) tends to adhere on the region with lower solid surface energy while droplet with higher surface tension (or weaker interaction with solid surface) prefer to stick on the area with higher solid surface energy. In this way, we can easily sort the liquid droplet according to the surface tension by using the superamphiphobic surface with gradient solid surface energy.

Fabrication and characterization of superamphiphobic surface

In order to obtain a superamphiphobic surface with tunable wettability (or solid surface energy), we firstly fabricate the superamphiphobic surface by using dual-size nanoparticles of titanium dioxide (TiO_2) coated with perfluorooctyltriethoxysilane according to previously reported method [24]. Two different size ranges of TiO_2 (~21 nm and ~60 to 200 nm) were simply mixed in an ethanol solution with perfluorooctyltriethoxysilane to obtain a milk-white suspension. Two different size ranges of TiO_2 were used to increase the roughness of the surface. This ethanol based suspension was sprayed on the clean glass surface (5 cm × 5 cm) and air-dried to fabricate the superamphiphobic surface. Scanning electron microscopy (SEM) images of the superamphiphobic surface show that the surface was composed of two different size ranges of TiO_2 nanoparticles (Fig. 1a). Energy dispersive spectrometer (EDS) (Fig. 1b) and X-ray photoelectron spectroscopy (XPS) (Fig. 1d) of the superamphiphobic surface showed that the TiO_2 nanoparticles on the surface were coated with perfluorooctyltriethoxysilane. The superamphiphobicity of the surface was evident from a range of liquid droplets beading up on the surface (Fig. 1c, top). The surface displayed very high apparent contact angles with water, glycerol, olive oil, and *n*-hexadecane (Fig. 1c, bottom) indicating that the surface is both superhydrophobic and superoleophobic, that is, superamphiphobic. The superamphiphobicity of the surface was further evident from water and diiodomethane liquid droplets bouncing on the surface as shown in Movie S1 (see, Electronic Supplementary Material (ESM)).

Tuning the superamphiphobic surface with gradient wettability

As mentioned above, the fabricated superamphiphobic surface was composed of two different size ranges of TiO_2 nanoparticles which were coated with perfluorooctyltriethoxysilane. TiO_2 nanoparticles, especially P25 TiO_2 nanoparticles, have high photocatalytic activity which could be used to precisely regulate the surface chemistry through UV irradiation-induced surface organic compounds degradation [25, 26]. Under UV irradiation ($\lambda = 365$ nm), electron-hole pairs generated on the

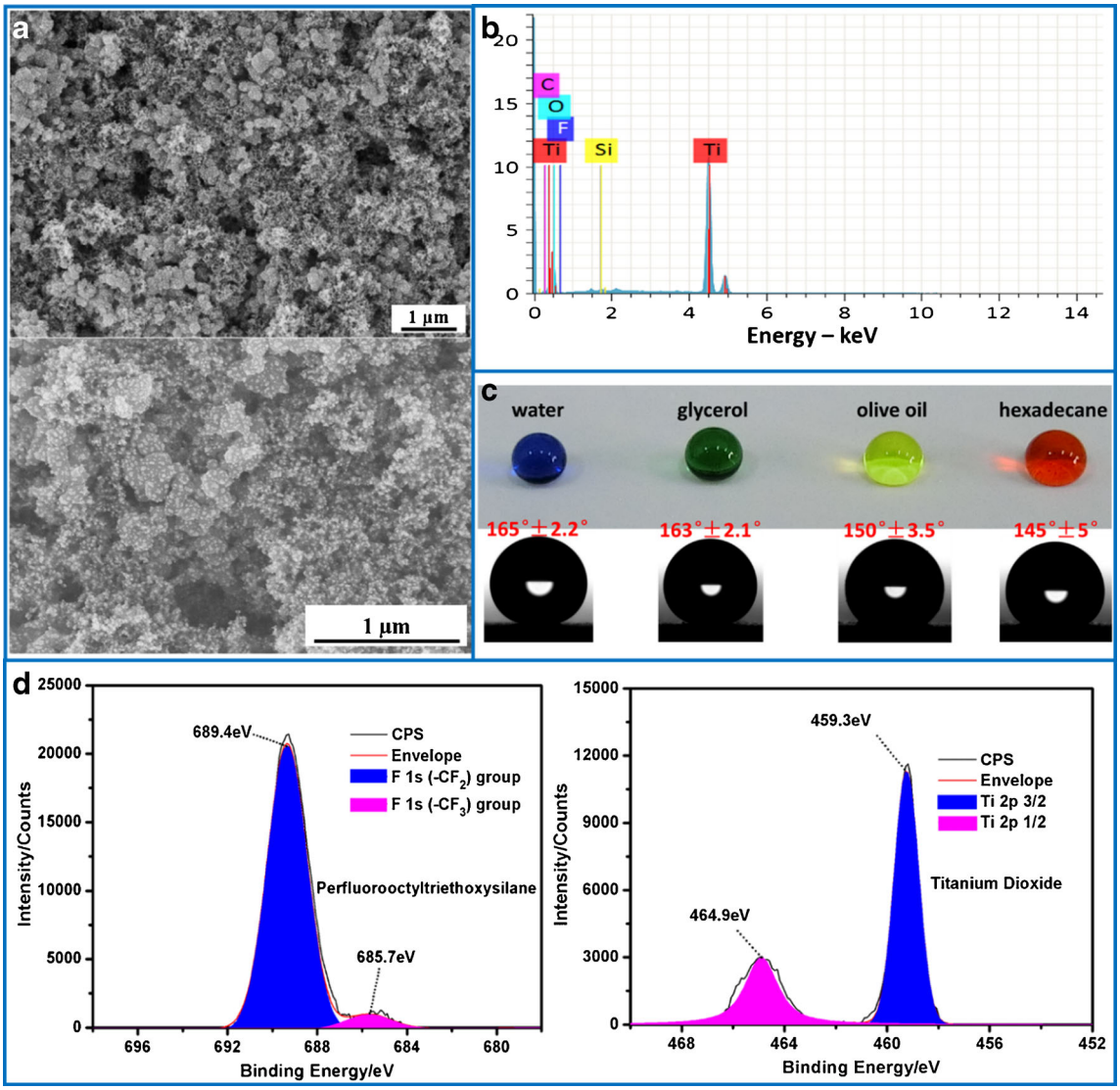

Fig. 1 Characterizations of the superamphiphobic TiO_2 surface. **a** Scanning electron microscope (SEM) images showing the constituent TiO_2 nanoparticles on the surface. Nanoparticles with small size (about 21 nm) refers to P25. **b** Energy dispersive spectrometer (EDS) showing the elemental compositions of the superamphiphobic TiO_2 surface. **c** Photographs of different droplets beading up on the superamphiphobic surface (top) and corresponding apparent contact angles (bottom). **d** X-ray photoelectron spectroscopy (XPS) of the superamphiphobic TiO_2 surface, where "Ti" refers to TiO_2 and "F" refers to perfluorooctyltriethoxysilane

surface of TiO_2 nanoparticles can produce radical species such as $\bullet O_2^-$ and •OH. These radical species could further degrade the organic compounds such as $-CF_2$ and $-CF_3$ groups in this system, resulting in the change of solid surface energy and wettability. Accordingly, the wettability (solid surface energy) of the superamphiphobic surface was finely tuned through gradient UV irradiation of the superamphiphobic surface as shown in Fig. 2a. The UV lightproof mask was placed above the superamphiphobic surface and was pushed forward at a constant speed by using the micro-injection pump. In this way, the superamphiphobic surface was gradiently UV irradiated. The UV irradiation gradient can be easily controlled through tuning the pump speed according to the length of the superamphiphobic surface. Here, we control the gradient UV irradiation time from 0 to 20 min, which means that the UV irradiation time linearly increased from 0 (at the initiating edge of the surface) to 20 min (at the end edge of the surface).

XPS was used to confirm the gradient degradation of $-CF_2$ and $-CF_3$ groups on the surface after gradient UV irradiation. As can be seen from Fig. 2b, the peak of $-CF_3$ disappeared after a 4-min irradiation and the peak of $-CF_2$ decreased with the increasing of UV irradiation time. The degradation of $-CF_2$ and $-CF_3$ groups resulted in the increase of surface energy. As shown in Fig. S1 (see ESM), the solid surface energy linearly increased with the increasing of UV irradiation time. Correspondingly, the apparent contact angles of ethanol with different concentrations decreased with the increasing of UV irradiation time (Fig. 2c). The droplet sorting ability of the UV irradiated surface was demonstrated by

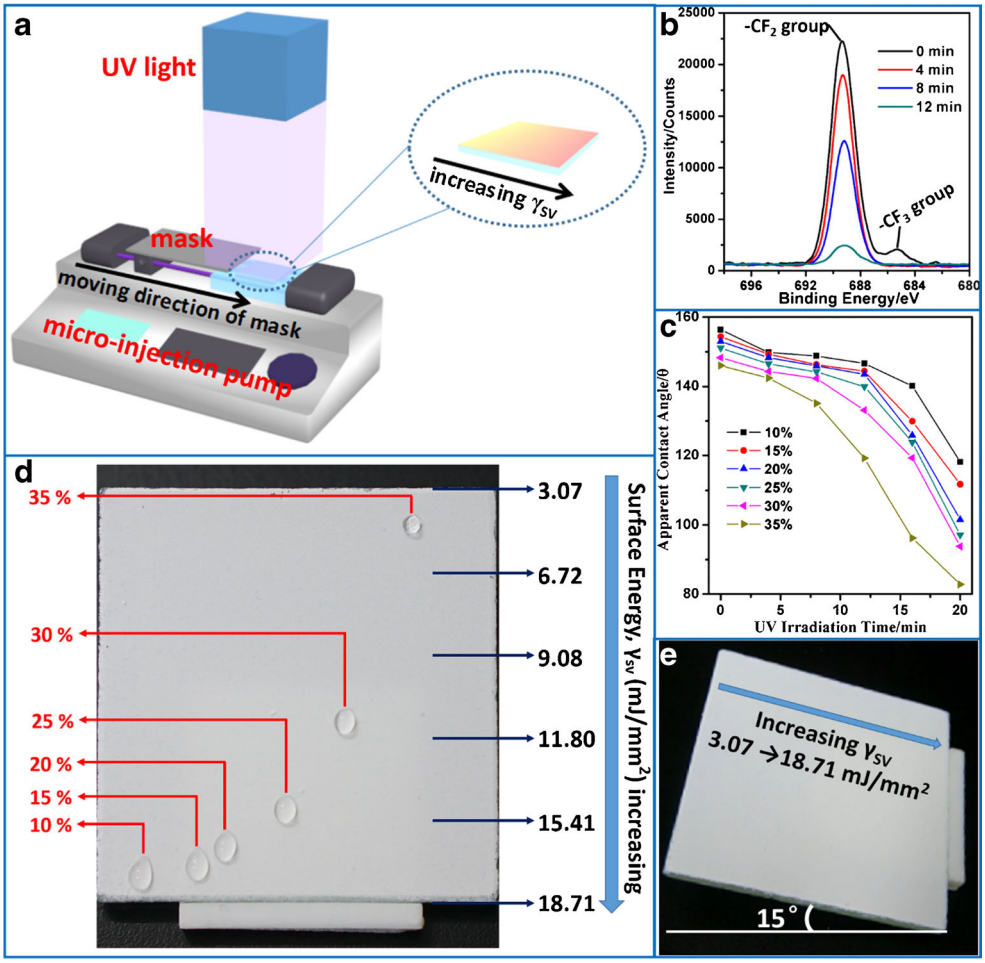

Fig. 2 **a** Schematic showing the process of tuning the wettability (solid surface energy) of the superamphiphobic surface. **b** X-ray photoelectron spectroscopy (XPS) of superamphiphobic surface with different UV irradiation times. **c** Apparent contact angles of ethanol with different concentrations on superamphiphobic surface decreasing with increasing UV irradiation time. **d** Liquid droplets with different surface tensions sticking on different position of the superamphiphobic surface with gradient wettability showing the liquid droplets sorting ability. **e** Image showing the fabricated surface leaning on the inclined plane with a 15° inclination

sorting six different droplets of ethanol with different concentrations or surface tensions (the corresponding surface tensions with different ethanol concentrations were shown in ESM Fig. S2) as shown in Fig. 2d. The UV irradiated surface was tilted at a fixed angle 15° with 0-min UV irradiation (low solid surface energy) at the top of the incline and 20-min UV irradiation (high solid surface energy) at the bottom of the incline. The UV irradiation time linearly increased from 0 to 20 min along the incline and also the solid surface energy linearly increased along the incline. The ethanol droplets with different concentrations were placed on top of the incline and let them freely roll off. As can be seen from Fig. 2d and ESM Movie S2, the ethanol droplet with low concentration can easily roll off from the top of the incline and adhere to the bottom area of the incline, while the ethanol droplet with high concentration trend to adhere to the top area of the incline. According to the position of the droplets, we can easily sort the ethanol droplets with different concentrations.

Biosensing applications for naked-eye ATP detection

The biosensing application of this superamphiphobic surface with gradient wettability was demonstrated using this surface to detect ATP. ATP is a general bacterial marker [27], naked-eye ATP detection has potential application for the detection of infectious organisms [28]. As a proof-of-concept, we used this surface to sort the liquid droplets after ATP-dependent DNA rolling circle amplification (RCA). In a typical process, 5′ phosphorylation modified linear ssDNA (5’-TCGTTTGATGTTCCTAACGT ACCAACGCACACGCAGTATTATGGACTGGTAAAAGC TTTCCGAGGTAGCCTGGAGCATAGAGGCATTGGCTG-3′) firstly annealed with primer DNA (5’-TAGGAACA TCAAACGACAGCCA-3′). The separated terminals of the linear ssDNA was then connected by T4 DNA ligase in the presence of ATP to form a circular DNA template (as shown in Fig. 3a). This circular DNA can further be used as template for RCA to form long single-stranded DNA product. Without the ATP, the linear ssDNA cannot be connected by T4 DNA ligase and no RCA product formed as shown in Fig. S3 (see, ESM). As the DNA ligase process is highly ATP-dependent [29], we tune the concentration of ATP to regulate the concentration of circular DNA template, which correspondingly regulate the concentration or length of RCA DNA product. The surface tensions of the liquids with different ATP concentrations after RCA decreased with the increasing of ATP concentration (ESM Fig. S4). After RCA with different concentrations of ATP, the liquid droplets of the product were placed on the tilted surface (with 15° tilt angle)

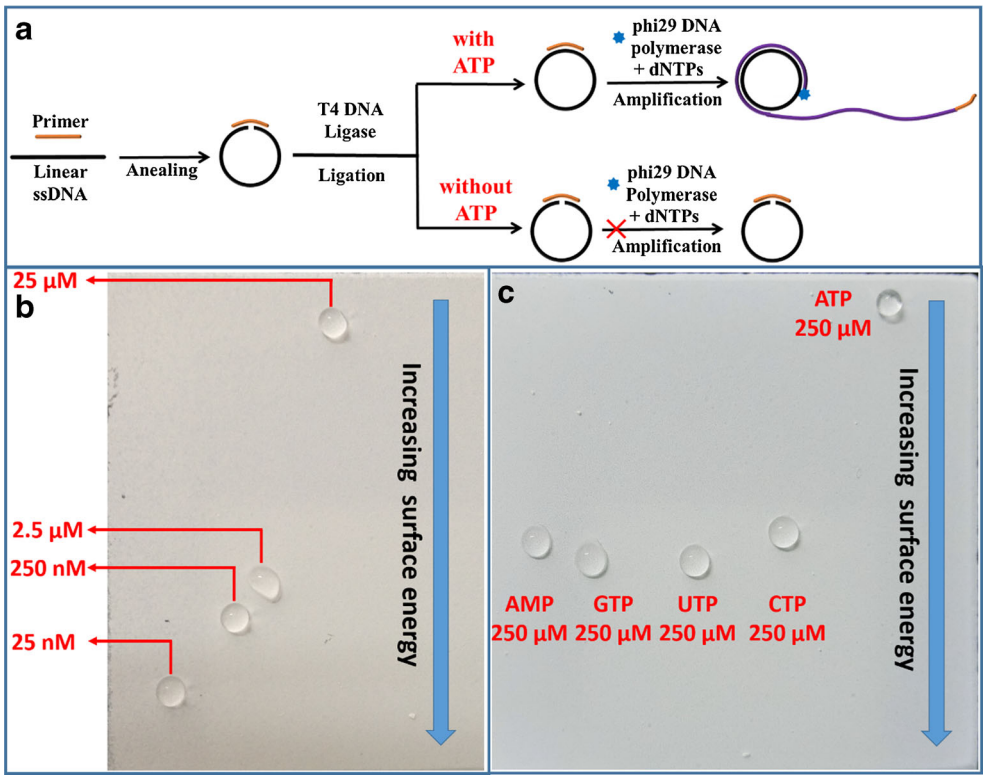

Fig. 3 **a** Schematic illustration of ATP-dependent rolling circle amplification. **b** Liquid droplets with different concentrations of ATP after rolling circle amplification sticking on different position on the surface. **c** Liquid droplets with AMP, GTP, UTP, CTP, and ATP after rolling circle amplification sticking on different position on the surface showing the specificity of ATP detection

and let them freely roll off from the top of the incline. As can been seen from Fig. 3b and ESM Movie S3, the droplet with low ATP concentration rolled off from the top of the incline easily and then adhered to the bottom area of the incline, while the droplet with high ATP concentration more likely to stick on the top area of the surface. According to the position of the droplet, we can easily discriminate the concentration of ATP. One thing should be point out is that the specificity of this ATP detection method was further demonstrated by using AMP, GTP, UTP, CTP, and ATP with 250 μM to perform the rolling circle amplification. After RCA, the droplets were sorted using the fabricated surface and the results were shown in Fig. 3c and ESM Movie S4. The results shows that the droplets with AMP, GTP, UTP, and CTP after RCA easily rolled off from the top of the incline, while the droplet with ATP adhered to the top of the incline. This excellent specificity was achieved because the process of DNA ligation is highly ATP-dependent and it is hard to form the circular DNA template for RCA without the ATP (ESM Fig. S4).

Conclusions

In summary, we demonstrated a method to fabricate superamphiphobic with gradient solid surface energy for naked-eye ATP detection. We fabricated superamphiphobic surface using two different size ranges of TiO_2 nanoparticles coated with perfluorooctyltriethoxysilane. The surface chemistry, and consequently the solid surface energy of this fabricated superamphiphobic was finely regulated through UV irradiation-induced organic compound degradation based on the high photocatalytic activity of TiO_2 nanoparticles. The superamphiphobic surface with gradient solid surface energy was obtained via gradient UV irradiation. We demonstrated the droplet-sorting ability of the fabricated surface by using it to discriminate ethanol droplets with different concentrations according to the position of droplets sticking on the tilted surface after rolling off from the top incline. The biosensor application of this superamphiphobic surface was preliminarily attempted to detect ATP combining ATP-dependent RCA with the droplet-sorting ability of the fabricated surface. The droplets with different concentrations of ATP after RCA can be effectively sorted and this ATP detection method showed good specificity. This developed methodology for droplet-sorting is energy-efficient and economical which is promising for biosensors, point-of-care testing, and biochemical assays.

Funding information This work is supported by the National Basic Research Program of China (973 Program, 2015CB932600), the National Key R&D Program of China (2017YFA0208000, 2016YFF0100800), the National Natural Science Foundation of China (21525523, 21722507, 21574048, 21874121), The Fok Ying-Tong Education Foundation, China (151011).

Compliance with ethical standards

Conflict of interest The authors declare that they have no competing interests.

References

1. Bhushan B, Jung YC, Koch K. Self-cleaning efficiency of artificial superhydrophobic surfaces. Langmuir. 2009;25(5):3240–8. https://doi.org/10.1021/la803860d.
2. Blossey R. Self-cleaning surfaces - virtual realities. Nat Mater. 2003;2(5):301–6. https://doi.org/10.1038/nmat856.
3. Furstner R, Barthlott W, Neinhuis C, Walzel P. Wetting and self-cleaning properties of artificial superhydrophobic surfaces. Langmuir. 2005;21(3):956–61. https://doi.org/10.1021/la0401011.
4. Zhang PC, Lin L, Zang DM, Guo XL, Liu MJ. Designing bioinspired anti-biofouling surfaces based on a superwettability strategy. Small. 2017;13(4). https://doi.org/10.1002/Smll.201503334.
5. Guo P, Zheng YM, Wen MX, Song C, Lin YC, Jiang L. Icephobic/anti-icing properties of micro/nanostructured surfaces. Adv Mater. 2012;24(19):2642–8. https://doi.org/10.1002/adma.201104412.
6. Cao LL, Jones AK, Sikka VK, Wu JZ, Gao D. Anti-icing superhydrophobic coatings. Langmuir. 2009;25(21):12444–8. https://doi.org/10.1021/la902882b.
7. Emelyanenko AM, Boinovich LB, Bezdomnikov AA, Chulkova EV, Emelyanenko KA. Reinforced superhydrophobic coating on silicone rubber for longstanding anti-icing performance in severe conditions. ACS Appl Mater Interfaces. 2017;9(28):24210–9. https://doi.org/10.1021/acsami.7b05549.
8. Zhang XY, Li Z, Liu KS, Jiang L. Bioinspired multifunctional foam with self-cleaning and oil/water separation. Adv Funct Mater. 2013;23(22):2881–6. https://doi.org/10.1002/adfm.201202662.
9. Ma QL, Cheng HF, Fane AG, Wang R, Zhang H. Recent development of advanced materials with special wettability for selective oil/water separation. Small. 2016;12(16):2186–202. https://doi.org/10.1002/smll.201503685.
10. Crick CR, Parkin IP. Water droplet bouncing-a definition for superhydrophobic surfaces. Chem Commun. 2011;47(44):12059–61. https://doi.org/10.1039/c1cc14749h.
11. Schutzius TM, Jung S, Maitra T, Graeber G, Kohme M, Poulikakos D. Spontaneous droplet trampolining on rigid superhydrophobic surfaces. Nature. 2015;527(7576):82–5. https://doi.org/10.1038/nature15738.
12. Draper MC, Crick CR, Orlickaite V, Turek VA, Parkin IP, Edel JB. Superhydrophobic surfaces as an on-chip microfluidic toolkit for total droplet control. Anal Chem. 2013;85(11):5405–10. https://doi.org/10.1021/ac303786s.
13. Yang XL, Liu X, Lu Y, Song JL, Huang S, Zhou SN, et al. Controllable water adhesion and anisotropic sliding on patterned superhydrophobic surface for droplet manipulation. J Phys Chem C. 2016;120(13):7233–40. https://doi.org/10.1021/acs.jpcc.6b02067.
14. Movafaghi S, Wang W, Metzger A, Williams DD, Williams JD, Kota AK. Tunable superomniphobic surfaces for sorting droplets by surface tension. Lab Chip. 2016;16(17):3204–9. https://doi.org/10.1039/c6lc00673f.
15. Zheng W, Jiang X. Integration of nanomaterials for colorimetric immunoassays with improved performance: a functional perspective. Analyst. 2016;141(4):1196–208. https://doi.org/10.1039/c5an02222c.
16. Zhou W, Gao X, Liu D, Chen X. Gold nanoparticles for in vitro diagnostics. Chem Rev. 2015;115(19):10575–636. https://doi.org/10.1021/acs.chemrev.5b00100.
17. Howes PD, Rana S, Stevens MM. Plasmonic nanomaterials for biodiagnostics. Chem Soc Rev. 2014;43(11):3835–53. https://doi.org/10.1039/c3cs60346f.
18. Tang L, Li J. Plasmon-based colorimetric nanosensors for ultrasensitive molecular diagnostics. ACS Sens. 2017;2(7):857–75. https://doi.org/10.1021/acs.sensors.7b00282.
19. Tian DL, Song YL, Jiang L. Patterning of controllable surface wettability for printing techniques. Chem Soc Rev. 2013;42(12):5184–209. https://doi.org/10.1039/c3cs35501b.
20. Cavallini M, Gentili D, Greco P, Valle F, Biscarini F. Micro- and nanopatterning by lithographically controlled wetting. Nat Protoc. 2012;7(9):1668–76. https://doi.org/10.1038/nprot.2012.094.
21. Lee H, Lee SG, Doyle PS. Photopatterned oil-reservoir micromodels with tailored wetting properties. Lab Chip. 2015;15(14):3047–55. https://doi.org/10.1039/c5lc00277j.
22. Lee KJ, Pan F, Carroll GT, Turro NJ, Koberstein JT. Photolithographic technique for direct photochemical modification and chemical micropatterning of surfaces. Langmuir. 2004;20(5):1812–8. https://doi.org/10.1021/la0358163.
23. Lafuma A, Quere D. Superhydrophobic states. Nat Mater. 2003;2(7):457–60. https://doi.org/10.1038/nmat924.
24. Lu Y, Sathasivam S, Song J, Crick CR, Carmalt CJ, Parkin IP. Robust self-cleaning surfaces that function when exposed to either air or oil. Science. 2015;347(6226):1132–5. https://doi.org/10.1126/science.aaa0946.
25. Yu JC, Yu JG, Ho WK, Zhang LZ. Preparation of highly photocatalytic active nano-sized TiO_2 particles via ultrasonic irradiation. Chem Commun. 2001;(19):1942–3. https://doi.org/10.1039/b105471f.
26. Zhang H, Lv XJ, Li YM, Wang Y, Li JH. P25-graphene composite as a high performance photocatalyst. ACS Nano. 2010;4(1):380–6. https://doi.org/10.1021/nn901221k.
27. Sassanfar M, Szostak JW. An RNA motif that binds ATP. Nature. 1993;364(6437):550–3. https://doi.org/10.1038/364550a0.
28. Hui CY, Liu M, Li YF, Brennan JD. A paper sensor printed with multifunctional bio/nano materials. Angew Chem Int Ed. 2018;57(17):4549–53. https://doi.org/10.1002/ange.201712903.
29. Ali MM, Li F, Zhang ZQ, Zhang KX, Kang DK, Ankrum JA, et al. Rolling circle amplification: a versatile tool for chemical biology, materials science and medicine. Chem Soc Rev. 2014;43(10):3324–41. https://doi.org/10.1039/c3cs60439j.